Turkish Journal of Electrical Engineering & Computer Sciences

http://journals.tubitak.gov.tr/elektrik/

Research Article

Turk J Elec Eng & Comp Sci
(2017) 25: 1388 – 1393

doi:10.3906/elk-1508-217

Tunable microstrip dual-band bandpass filter for WLAN applications

Abbas REZAEI[1,*], **Leila NOORI**[2]

[1]Department of Electrical Engineering, Kermanshah University of Technology, Kermanshah, Iran

[2]Young Researchers and Elite Club, Kermanshah Branch, Islamic Azad University, Kermanshah, Iran

Received: 25.08.2015 • **Accepted/Published Online:** 11.05.2016 • **Final Version:** 10.04.2017

Abstract: In this paper, based on a new stub-loaded open loop resonator, a compact microstrip dual-band bandpass filter is presented. The proposed filter is designed using two stub-loaded open loop resonators to create two pass bands at 2.39 GHz and 5.7 GHz for multimode wireless LANs applications. Two high impedance sections are used in the main loops and the internal stubs are two low impedance microstrip cells. A method is presented to control the mode resonance frequencies. By increasing the internal stubs' dimensions, the resonance frequencies are adjusted without size increment. The proposed filter has a good performance. The insertion losses at 2.39 GHz and 5.7 GHz frequencies are 0.1 dB and 0.4 dB, respectively, while the return loss at the two pass bands is better than –16.6 dB. The filter size is 251 mm^2. The designed filter is fabricated and measured. The results show that there is a good agreement between the simulation and measurement.

Key words: Microstrip, dual-band, resonance frequency, open loop, bandpass filter

1. Introduction

The wireless local area network has become the most important communication technology. Dual-band and even tri-band systems are employed in these ubiquitous wireless communications [1]. Dual-band filters operated at 2.4 GHz/5.2 GHz and 2.4 GHz/5.7 GHz are used in wireless local area network applications. In [2–11] dual-band bandpass filters with large dimensions and large insertion losses have been presented. In [2] a dual-band bandpass filter has been designed to create two pass bands at 2.4 GHz/5.2 GHz, using $\lambda/2$ stepped-impedance resonators and distributed parallel-coupled microstrip lines, but the selectivity of this filter is not good. In [3] a dual-band bandpass filter in low-temperature co-fired ceramic technology has been fabricated to create two pass bands at 2.4 GHz/5.2 GHz. However, it has an undesired isolation between two pass bands. In [4] a dual-band bandpass filter using the step impedance resonator with three transmission zeroes has been presented. In this structure, taped line feed structures have been used to match the impedance and to improve the insertion loss, which lead to increased filter size. To achieve a dual-band bandpass filter in [5], a step impedance resonator with very large implementation area has been used. In [6] a complex dual-band bandpass filter has been designed based on a dual-plane structure consisting of a microstrip and a defected ground structure slot. In [7] a dual-band band pass filter with a complex structure has been introduced. In [8] a step impedance resonator with very large dimension has been used to obtain a dual-band bandpass response for ultra-wideband applications. In [9–11], open loop resonators have been used to achieve dual-band bandpass filters. In [9] half wave step impedance resonators have been used with undesired selectivity. In [10] three different dual-band bandpass filters have been

*Correspondence: unrezaei@yahoo.com

designed. In two of them, four open loop resonators have been used, which lead to size increment. Moreover, large tapped-line feed structures have been used, which lead to increase in size of the filters. In [11] four open loop resonators have been connected together for ultra-wideband applications.

In this paper, a tunable dual-band bandpass filter is designed using two stub-loaded open loop resonators to solve the previous works' problems such as large size, large insertion loss, large return loss, and undesired selectivity.

2. Filter structure

A high-impedance and a low-impedance section are shown in Figures 1a and 1b, respectively. An open loop resonator is presented in Figure 1c. The proposed resonator consists of a high-impedance section (similar to Figure 1a) loaded by a low impedance cell (similar to Figure 1b). In Figure 1c, θ_i and y_i are the electrical length and characteristic admittance, respectively, related to the physical length l_i, where i = 1, 2a, 2b, 3, 4a, 4b, 5, 6, 7, 8, 9, 10, 11.

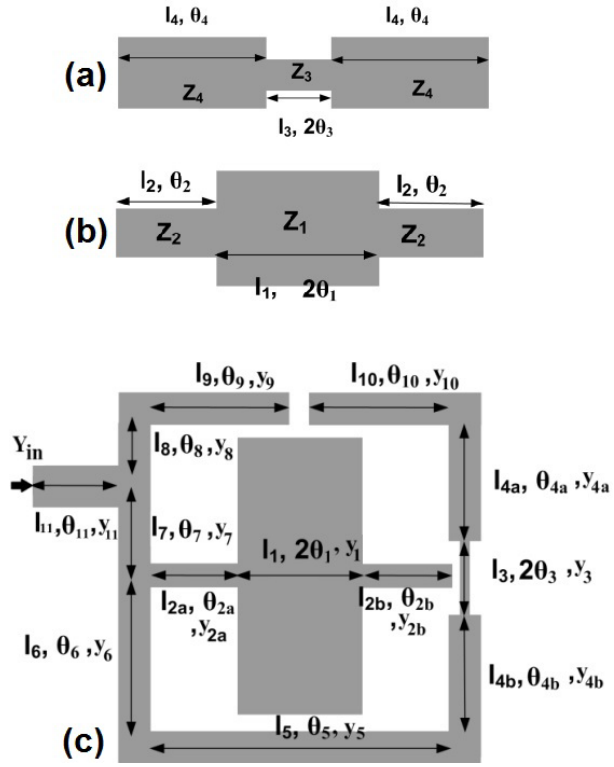

Figure 1. (a) High impedance section, (b) low impedance section, (c) proposed resonator.

According to the transmission line theory, the input admittance of an open-circuited transmission line with the characteristic admittances y_i is given by

$$y_{in} = j\, y_i \tan(\theta_i) \quad \text{for } i = A,\ B,\ S, \text{ and } 11 \tag{1a}$$

where

$$\frac{1}{y_A} = \frac{1}{y_{10}} + \frac{1}{y_{4a}} + \frac{1}{y_3} + \frac{1}{y_{4b}} + \frac{1}{y_5} + \frac{1}{y_6} \tag{1b}$$

$$\frac{1}{y_S} = \frac{1}{y_{2a}} + \frac{1}{y_1} + \frac{1}{y_{2b}} \tag{1c}$$

$$\frac{1}{y_B} = \frac{1}{y_9} + \frac{1}{y_8} \tag{1d}$$

The input admittance of the proposed resonator viewed from the input port Y_{in} is

$$Y_{in} = \frac{\left[\frac{(y_S + y_A)\, y_7}{y_S + y_A + y_7} + y_B\right] y_{11}}{\frac{(y_S + y_A)\, y_7}{y_S + y_A + y_7} + y_B + y_{11}} \tag{2}$$

The resonance frequencies are obtained when $Y_{in} = 0$ and/or $Z_{in} = \frac{1}{Y_{in}} = 0$. Therefore, from Eqs. (1.a) and (2) the resonance conditions are obtained as follows:

$$y_B tan\left(\theta_B\right) = -\frac{\left[y_S tan\left(\theta_S\right) + y_A tan\left(\theta_A\right)\right] y_7}{y_S tan\left(\theta_S\right) + y_A tan\left(\theta_A\right) + y_7} \tag{3a}$$

$$y_{11} tan\left(\theta_{11}\right) = 0 \tag{3b}$$

There are several solutions for Eqs. (3a) and (3b). From Eq. (3a) a method to control the resonance frequencies can be found with changing of the electrical lengths θ_S, θ_A, and θ_B. While the electrical lengths have a direct relation with the physical lengths, by tuning the physical lengths and widths of the internal stubs and loop dimension, two desired resonance frequencies can be obtained. A useful method to control the resonance frequency and miniaturization is to increase the internal stubs and to decrease the loop size, which leads to decreased resonator dimensions. From Eq. (3a), to increase the internal stubs and to decrease the loop size, θ_S must be increased, while θ_A is decreased and θ_B is a constant parameter.

From Eq. (3b), if $\theta_{11} = \pi$, for a resonance frequency $f_r = 5.2$ GHz and a substrate with the effective dielectric constant $\varepsilon_{re} = 2.2$, we have the guided wavelength $\lambda_g = 38.8$ and $l_{11} = 19.4$ mm. This obtained dimension of l_{11} leads to size increment. Therefore, two similar resonators can be connected together to reduce the dimension of the tapped line.

The resonance conditions for the reflection zeroes can be obtained when $Z_{in} = \frac{1}{Y_{in}} = 0$. Under this condition, the resonance condition is

$$\frac{(y_S + y_A)\, y_7}{y_S + y_A + y_7} + y_B + y_{11} = 0 \tag{4}$$

From Eq. (4), the resonance frequency can be tuned by adjusting y_s as a function of y_A, y_B, y_7, and y_{11}. Therefore, the resonance frequency can be tuned by selecting the loop dimensions and then the internal stub as a function of the loop dimensions.

Two open loop resonators as shown in Figure 1c are coupled together to form the proposed filter as shown in Figure 2a. The proposed filter has a dual-band bandpass response with controllable resonance frequencies and a low loss. The frequency response of the proposed filter is shown in Figure 2b. While an electrical length has a direct relation with the propagation constant (β) (propagation constant depends on the effective dielectric

constant (ε_{re}) and ε_{re} is related to the width [12]), the effects of the widths on the resonance frequency are clear. The effects of the length l_6 and the width w_5 on the resonance frequencies are shown in Figures 2c and 2d, respectively. By decreasing the length l_6, the first resonance frequency is shifted to the right (higher frequencies) and by increasing the width w_5, the first and second resonance frequencies are shifted to the left. As shown in Figure 2e, by increasing the space S, the insertion losses at the both pass bands are increased. The proposed filter is fabricated and its photograph is shown in Figure 2f.

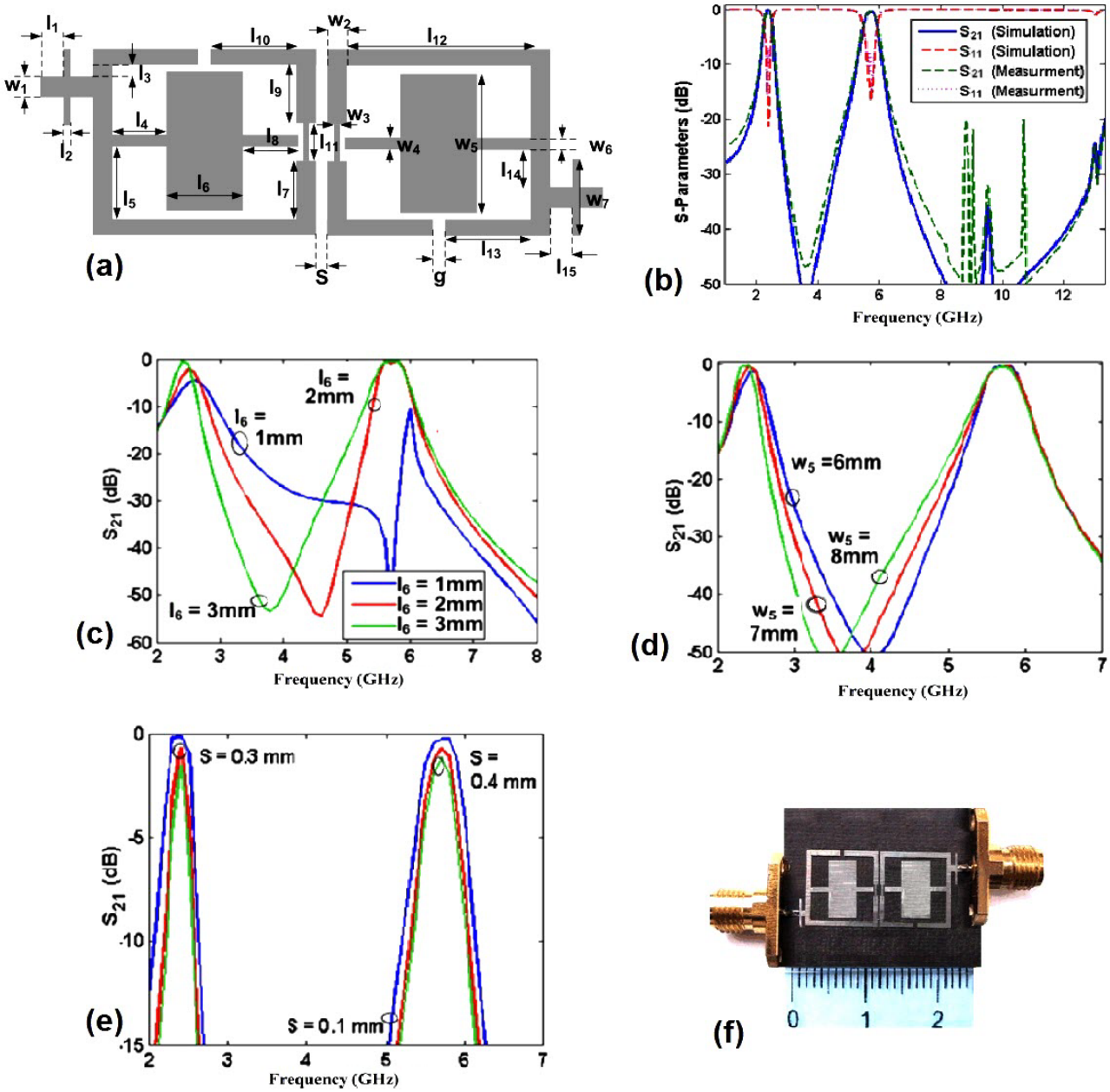

Figure 2. (a) The proposed filter using the high and low-impedance sections, (b) frequency response of the proposed filter, (c) frequency response as a function of the length l_6, (d) frequency response as a function of w_5, (e) frequency response as a function of S, (f) photograph of the fabricated filter.

3. Results

The proposed filter is simulated using the full wave EM simulator and fabricated on a RT Duroid 5880 substrate with the dielectric constant $\varepsilon_r = 2.22$, 15-mil thickness, and loss tangent 0.0009. The dimensions of the proposed filter per mm are (see Figure 2a): $l_1 = 1$, $l_2 = 0.3$, $l_3 = 0.6$, $l_4 = 2.4$, $l_5 = 3.9$, $l_6 = 3.4$, $l_7 = 3.2$, $l_8 = 2.4$, $l_9 = 3.2$, $l_{10} = 3.8$, $l_{11} = 2$, $l_{12} = 8.1$, $l_{13} = 3.8$, $l_{14} = 2$, $l_{15} = 1$, $w_1 = 1.2$, $w_2 = 0.9$, $w_3 = 0.3$, $w_4 = 0.7$, $w_5 = 7.6$, $w_6 = 0.7$, $w_7 = 4.2$, S = 0.2, and g = 0.5. This filter has cut-off frequencies at 2.26 GHz and 2.52 GHz in the first band and 5.47 GHz and 5.92 GHz in the second band. Below the first pass band the minimum attenuation is –20 dB from DC to 1.82 GHz. Between two pass bands the minimum attenuation is –20 dB from 2.74 GHz to 4.92 GHz. The worst value of the harmonic above the second pass band is –20 dB from 6.36 GHz to 13.3 GHz. The insertion losses at 2.39 GHz and 5.7 GHz are better than 0.1 dB and 0.4 dB, respectively, while the return losses in the first and the second pass band are better than 21.3 dB and 16.6 dB, respectively. The filter size is 24.6 $\times$ 10.2 mm^2. In comparison to the previous works, the filter size is small and the insertion loss is good. The fractional bandwidths in the first and second bands are 10.8% and 7.9%, respectively. A comparison between the designed filter and the previous works is shown in the Table. In the Table, IL1, IL2, RL1, RL2, F_{o1}, and F_{o2} are the first band insertion loss, the second band insertion loss, the first band return loss, the second band return loss, the first resonance frequency, and the second resonance frequency, respectively. From the Table it is clear that the designed filter not only has a smaller size but also has good performances in terms of insertion loss, return loss, fractional bandwidth, and selectivity.

Table. Comparison between the proposed filter and the previous works.

Ref.	IL1 (dB)	IL2 (dB)	RL1 (dB)	RL2 (dB)	F_{O1} (GHz)	F_{02} (GHz)	Size (mm^2)
This work	0.1	0.4	21.3	16.6	2.39	5.7	251
[1]	6	5.3	—	—	2.42	5.24	434
[5]	1.8	3	—	—	2.45	5.8	2600
[7]	2.65	2.44	12.6	12.6	1	2	1325
[8]	2.12	2.33	12	12	2.45	5.8	1905
[9]	1.85	1.9	—	—	2.46	5.6	311
[10]	1.87	1.67	—	—	2.44	5.75	655
[11]	0.2	0.9	—	—	2.71	5.05	495
[13]	0.3	0.7	12	10	2.65	7.85	299
[14]	0.52	0.84	25.3	17.9	2.4	4	391
[15]	0.53	0.59	10	13.4	2.4	5.2	320

4. Conclusion

In this paper, a miniaturized dual-band bandpass filter with tunable resonance frequencies is designed and fabricated for high-speed WLANs. The conditions of the even mode resonance frequencies are obtained to tune the resonance frequencies without size increment. In comparison with previous works, the insertion losses in both the first and second bands are small while the return losses are reasonable. The harmonics above the second pass band are attenuated from 6.36 GHz to 13.3 GHz with the minimum attenuation of –20 dB.

References

[1] Lee HM, Tsai CC. Dual-band filter design with flexible pass band frequency and bandwidth selections. IEEE T Microw Theory 2007; 55: 1002-1009.

[2] Sun S, Zhu L. Coupling dispersion of parallel coupled microstrip lines for dual-band filters with controllable fractional pass bandwidths. IEEE MTT-S Int Microw Symp Dig 2005; 4: 2195-2198.

[3] Zhang YP, Sun M. Dual-band microstrip bandpass filter using stepped-impedance resonators with new coupling scheme. IEEE T Microw Theory 2006; 54: 3779-3785.

[4] Weng MH, Wu HW, Su YK. Compact and low loss dualband bandpass filter using pseudo-interdigital stepped impedance resonators for WLANs. IEEE Microw Wireless Compon Lett 2007; 17: 187-189.

[5] Kuo JT, Yeh TH, Yeh CC. Design of microstrip bandpass filters with a dual-pass band response. IEEE T Microw Theory 2005; 53: 1331-1337.

[6] Ren L, Huang H. Dual-band bandpass filter based on dual-plane microstrip/interdigital DGS slot structure. Electron Lett 2009; 45: 1077-1079.

[7] Tseng CH, Shao HY. A new dual-band microstrip bandpass filter using net-type resonators. IEEE Microw Wireless Compon Lett 2010; 20: 196-198.

[8] Jiang M, Chang LM, Chin A. Design of dual-pass band microstrip bandpass filters with multi-spurious suppression. Microw Wireless Compon Lett 2010; 20: 199-201.

[9] Chen X, Han G, Ma R, Gao J, Zhang W. Design of balanced dual-band bandpass filter with self-feedback structure. ETRI J 2009; 31: 475-477.

[10] Mondal P, Mandal MK. Design of dual-band bandpass filters using stub-loaded open-loop resonators. IEEE T Microw Theory 2008; 56: 150-155.

[11] Hayati M, Noori L. Compact dual-band bandpass filter with ultra wide stopband using open loop resonator loaded by T-shape and open stubs. IEICE 2011; 8: 1168-1173.

[12] Hong JS, Lancaster M J. Microstrip Filters for RF/Microwave Applications. 2nd ed. New York, NY, USA: Wiley, 2001.

[13] Marimuthu J, Abbosh AM, Henin B. Planar microstrip bandpass filter with wide dual-bands using parallel-coupled lines and stepped impedance resonators. Prog Electromagn Res C 2013; 35: 49-60.

[14] Khajavi N, Makki S, Majidifar S. Design of high performance microstrip dual-band bandpass filter. Radioeng 2015; 24: 32-38.

[15] Hayati M, Noori L, Adinehvand A. Compact dual-band bandpass filter using open loop resonator for multimode WLANs. Electron Lett 2012; 48.